

See discussions, stats, and author profiles for this publication at: <https://www.researchgate.net/publication/268280953>

# Docking and Free Energy Perturbation Studies of Ligand Binding in the Kappa Opioid Receptor

ARTICLE in THE JOURNAL OF PHYSICAL CHEMISTRY B · NOVEMBER 2014

Impact Factor: 3.3 · DOI: 10.1021/jp5053612 · Source: PubMed

CITATIONS

2

READS

51

7 AUTHORS, INCLUDING:



**Robert B Murphy**

Schrodinger

32 PUBLICATIONS 7,819 CITATIONS

SEE PROFILE



**Lingle Wang**

Columbia University

14 PUBLICATIONS 268 CITATIONS

SEE PROFILE



**Thijs Beuming**

Schrodinger

40 PUBLICATIONS 1,456 CITATIONS

SEE PROFILE



**Robert Abel**

Schrodinger

22 PUBLICATIONS 3,060 CITATIONS

SEE PROFILE

# Docking and Free Energy Perturbation Studies of Ligand Binding in the Kappa Opioid Receptor

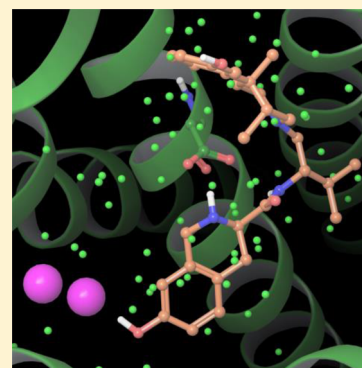
Dahlia A. Goldfeld,<sup>†,§</sup> Robert Murphy,<sup>‡</sup> Byungchan Kim,<sup>‡</sup> Lingle Wang,<sup>‡</sup> Thijs Beuming,<sup>‡</sup> Robert Abel,<sup>‡</sup> and Richard A. Friesner<sup>\*,†</sup>

<sup>†</sup>Department of Chemistry, Columbia University, 3000 Broadway, MC 3110, New York, New York 10027, United States

<sup>‡</sup>Schrödinger, Inc., New York, New York 10036, United States

## S Supporting Information

**ABSTRACT:** The kappa opioid receptor (KOR) is an important target for pain and depression therapeutics that lack harmful and addictive qualities of existing medications. We present a model for the binding of morphinan ligands and JDTic to the JDTic/KOR crystal structure based on an atomic level description of the water structure within its active site. The model contains two key interaction motifs that are supported by experimental evidence. The first is the formation of a salt bridge between the ligand and Asp 138<sup>3,32</sup> in transmembrane domain (TM) 3. The second is the stabilization by the ligand of two high energy, isolated, and ice-like waters near TM5 and TM6. This model is incorporated via energetic terms into a new empirical scoring function, WScore, designed to assess interactions between ligands and localized water in a binding site. Pairing WScore with the docking program Glide discriminates known active KOR ligands from large sets of decoy molecules much better than Glide's older generation scoring functions, SP and XP. We also use rigorous free energy perturbation calculations to provide evidence for the proposed mechanism of interaction between ligands and KOR. The molecular description of ligand binding in KOR should provide a good starting point for future drug discovery efforts for this receptor.



## INTRODUCTION

Opioids are among the most widely prescribed and abused pharmaceuticals, due to their powerful painkilling, antidepressant, and addictive properties.<sup>1,2</sup> People have extracted opium from the *Papaver somniferum* plant for millennia to garner these therapeutic attributes. In addition, when used in a clinical setting, opioids have severe side effects ranging from respiratory depression to dysphoria, which has motivated efforts to discover safer and nonaddictive medications.<sup>1</sup> Many synthetic opioids bind promiscuously to the  $\mu$ ,  $\delta$ , and  $\kappa$  opioid receptors (MOR, DOR, and KOR, respectively), and it is known that MOR is involved in the addiction pathway.<sup>3–8</sup> It is hoped that KOR and DOR selective, high-affinity ligands could be less addictive pharmaceutical options. KOR agonists have demonstrated desired pharmaceutical effects, while avoiding activation of reward pathways, although to date they do not avoid adverse effects like dysphoria. However, dysphoria appears to be triggered by arrestin recruitment to activate the receptor, and G-protein biased KOR ligands have been developed to avoid this pathway.<sup>9–11</sup> Like all structure based drug design efforts, further development of such compounds can benefit from a detailed molecular picture of how opioids bind to their receptors.

Creation of such a picture is now possible, as the kappa opioid receptor was crystallized in 2012 bound to the antagonist JDTic ((3R)-1,2,3,4-tetrahydro-7-hydroxy-N-[(1S)-1-[[[3R,4R)-4-(3-hydroxyphenyl)-3,4-dimethyl-1-piperidinyl]-methyl]-2-methylpropyl]-3-isoquinolinecarboxamide).<sup>12</sup> We

also have access to the three other opioid receptor structures—MOR, DOR, and the nociceptin/orphanin FQ peptide receptor—which, like KOR, all belong to the class A gamma subfamily of G-protein coupled receptors (GPCRs).<sup>13–16</sup> The KOR, DOR, and MOR subtypes are highly homologous, exhibiting around 70% sequence identity in the transmembrane (TM) region, which houses nonpeptidic ligands. These crystal structures are a major step forward toward developing a molecular understanding of opioid receptor recognition and selectivity.

With this in mind, we used the new KOR (PDB ID 4DJH) crystal structure to construct a hypothesis which applies to how the receptor binds JDTic and morphinan antagonists. Our hypothesis is based on the presence of localized waters within the binding site and the more negative binding free energy that comes from displacing them in a favorable way. We integrated the key elements of this hypothesis as terms in a new scoring function, WScore,<sup>17</sup> which allows us to distinguish between known active antagonists from a set of chemically similar decoys in virtual screening (VS) calculations. WScore was preliminarily described in ref 17 but has been expanded and further tested since then. The terms described in this paper that

**Special Issue:** William L. Jorgensen Festschrift

**Received:** May 30, 2014

**Revised:** November 12, 2014

**Published:** November 14, 2014

are necessary to accurately capture ligand binding in KOR represent part of the development of WScore over the past few years. The key features of WScore include integration of WaterMap into the Glide docking program and a variety of penalty terms which address desolvation and strain energy. These terms rely on both the location and displacement free energy characterization of quasilocalized water molecules in the active site of the receptor provided by running a WaterMap simulation. A full description of the current WScore scoring function and its validation will be presented in subsequent publications.

We briefly discuss several other recent approaches which have attempted to incorporate water structure into a description of ligand binding. Over the past several years, a number of other workers have introduced explicit water molecules<sup>18,19</sup> into a docking calculation. These approaches differ from WScore in that (a) the water positions are obtained from X-ray crystallographic experiments rather than simulations (which typically results in a less complete description of the active site water structure), (b) the displacement free energies are not available and hence cannot be used in developing the scoring function, (c) the details as to how the water molecules are incorporated into binding energy prediction are quite different from how this is accomplished in WScore. More extensive comparison of WScore with these alternative approaches will be provided in the follow on work describing WScore. The HYDE<sup>20</sup> scoring function<sup>20</sup> contains a comprehensive approach to desolvation; however, this utilizes an implicit solvent model, as opposed to the explicit waters employed in WScore. Assessment of the performance of HYDE vs WScore requires comparisons over a wide range of receptors and ligands, a task we reserve for another publication. Finally, Mason and co-workers<sup>21</sup> have used WaterMap and other programs (SZMAP, GRID), which provide insight into active site water structure and binding affinity to investigate ligand binding in a number of GPCR active sites (although not KOR). They obtain physical insights that are similar in character to what we find herein; however, they do not augment the information obtained by analyzing ligand–water interactions with the multiplicity of additional terms required to model the various relevant contributions to binding affinity (e.g., strain energy), and hence have not produced a complete scoring function along the lines of WScore.

We have also used free energy perturbation (FEP) calculations,<sup>22–24</sup> performed by way of explicitly solvated molecular dynamics (MD) simulations, as another way to describe the thermodynamics of JDTic binding, and the relative binding of JDTic derivatives, which can be compared with results from the empirical WScore scoring function and in some cases with experimental data. FEP produces accurate and rigorous thermodynamics predictions within the limits of force field accuracy and complete sampling of phase space. In general, consistency among results from docking calculations, which are quick and heuristic, FEP simulations, and experimental data lends confidence to the docking methodology. In this vein, we investigate our model of ligand binding to KOR and the key factors controlling binding affinity using WScore, FEP simulations, and experimental data. Further calculations and experiments will be required to fully confirm the proposed model.

Virtual screening to find drug leads against GPCRs is a popular line of research. Recent efforts based on new GPCR structures has resulted in useful results for the adenosine

A<sub>2A</sub>,<sup>25–27</sup> CXCR4,<sup>28</sup> M2 and M3,<sup>29</sup> H1,<sup>30</sup> and  $\beta$ 2-adrenergic<sup>31</sup> receptors, where many nM hits have been found computationally and several confirmed experimentally. However, KOR virtual screening has been more challenging. For example, Negri et al.<sup>32</sup> employed the DOCK (29) program to screen ligands against KOR and assayed 22 of the docking hits experimentally, but only a few very weak (120  $\mu$ M at best) KOR binders were found. This is consistent with the poor results we obtain using the standard Glide XP and SP scoring function in a retrospective virtual screening exercise, as is discussed below.

In this paper, we first present our improved model of binding in the context of the water structure in the KOR binding site, and explain how it was integrated into the widely used docking program, Glide,<sup>33–35</sup> via WScore. We then show how WScore greatly outperforms Glide SP and Glide XP in retrieving known actives from a database of similar (by construction) molecules whose activities have not been established. Finally, we present our FEP results and discuss them in the context of the WScore results, for which they provide support as noted above.

## ■ THEORETICAL METHODS

**1. Protein Preparation.** The crystal structure was prepared using the Protein Prep Wizard in the Schrödinger suite.<sup>36</sup>

**2. Ligand Preparation.** All actives and decoys were obtained from the Cavasotto GPCR Ligand Library and Decoy Database (GLL/GDD).<sup>37</sup> The protonation states were generated using LigPrep.<sup>38</sup>

**3. Glide Calculations.** For SP and XP calculations, the default 10 Å box and grid generation options were used. Flexible docking was performed using Glide SP and Glide XP without any constraints.

**4. WaterMap.** WaterMap<sup>39,40</sup> was used to generate the crystal water structure within KOR and MOR. First the proteins were prepared with the Protein Preparation Wizard in Maestro<sup>36</sup> and missing side chains were optimized with Prime.<sup>41</sup> WaterMap was run in the default mode; the cocrystallized ligands associated with each protein were used to define the binding site area and were removed during the MD simulations of the water structure.

**5. WScore.** WScore is a docking and scoring methodology that has been constructed by integrating WaterMap into the Glide docking program, using the explicit waters obtained from the WaterMap simulations to estimate water desolvation and trapping effects.<sup>17</sup> The WaterMap file that we calculated is provided in the Supporting Information file titled water-map\_wm.mae. We provide a brief summary here of key theoretical and practical aspects of the WaterMap methodology that are relevant to WScore. Much more extensive discussions along these lines, including many details not presented below, can be found in refs 39 and 40.

In a WaterMap calculation, an explicit solvent molecular dynamics calculation is performed for solvated protein (generally with the ligand removed, as is the case for WScore applications), with the protein coordinates harmonically restrained to the crystal structure coordinates in order to minimize noise. A clustering analysis of the trajectory yields regions of high water density; these regions are identified as sites of quasilocalized water occupation. A modified version of inhomogeneous solvation theory<sup>42,43</sup> is used to assign the displacement free energy (the free energy of transferring the water molecule into bulk solution, ignoring concentration effects which are discussed below) of a water molecule at each

of these sites. The displacement free energies can in many cases be correlated with experimental binding free energies, as has been done in a number of previous publications (e.g., ref 39). The occupation of a given site in the protein by a water molecule depends upon the displacement free energy defined above but also on the concentration of water in the surrounding solvent (55 M under normal biological conditions). Therefore, many sites with highly unfavorable free energies relative to bulk have very high occupation probabilities, due to the usual concentration effects manifested in the equations of equilibrium thermodynamics. An unfavorable displacement free energy of more than  $\sim 6$  kcal/mol is required before significant probability of a void in the site is observed.<sup>44</sup> In prior work, we have found a small number of receptors in the PDB where voids occur in molecular dynamics simulations (and presumably in the physical system as well); in the vast majority of cases, however, such unfavorable sites are occupied by a water molecule with a high probability.

In WScore, the water locations and displacement free energies derived from the WaterMap simulation are integrated into the Glide docking grid and used to estimate penalties for water desolvation and trapping. Several examples of our implementation, for the terms that are most relevant to KOR molecular recognition, are discussed below. A general exposition of our approach to the construction of this component of the scoring function will be presented in a future publication.

The scoring function is built on the Glide XP scoring function but includes new terms for strain energy, and optimization of Glide XP parameters, in addition to the more accurate treatment of desolvation and trapping effects discussed above. The sampling algorithms in WScore involve considerable additional sampling as compared to Glide XP, as higher resolution pose prediction is necessary in order for active compounds to avoid the substantial number of penalty terms that have been added to the scoring function.

WScore is designed to be used for any protein target of interest, but in this paper, we focus specifically on the key terms in WScore that make docking to KOR more accurate. There are two such critical terms: the term penalizing desolvation of Asp 138 and the term penalizing disruption (without compensatory hydrogen bonds with the ligand) of an unusual water structure comprised by two particular WaterMap waters. The physical chemistry underlying these two terms is elaborated upon in the "Model of Ligand Binding in the Kappa Opioid Receptor" section. Detailed technical descriptions of these terms follow. These terms are responsible for penalizing a significant fraction of the decoy ligands and hence for much of the success of WScore in improving enrichment. These terms, in combination with an alternative scoring function such as Glide XP, would in fact likely yield greatly improved enrichment results for KOR as well.

First we describe the WScore algorithm for evaluating desolvation of charged side chain groups such as Asp upon ligand binding. The first step is to determine the set of first shell WaterMap waters solvating the charged atoms of the side chain. The WaterMap waters are determined using the protein in the ligated conformation with the ligand removed and therefore represent solvation of the charged group before ligation in the sense of a thermodynamic cycle. First shell WaterMap water candidates are within 3.5 Å of the charged protein atoms and at a reasonable H bonding orientation to the charged group's H bonding electron density. For the case of a carboxylate group,

the  $\text{O}^- \rightarrow \text{WaterMap}$  water vector must have a dot product of more than 0.2 with the vector bisecting the two  $\text{O}^-$  atoms from the C of the  $\text{CO}_2^-$ . This provides a rough estimate of being in range of the  $\text{CO}_2^-$  negative charge density. Each first shell water of the charged group is tested for removal by the presence of the ligand. The removal fraction " $w_{\text{vac}}(i)$ " of a given water,  $i$ , is a function of its van der Waals (VdW) overlap with the ligand atoms

$$w_{\text{vac}}(i) = \min \left( 1.0, \sum_j 1.0 - \sqrt{\frac{d_{ij}}{r_{ij}}} \right) \quad \text{for } d_{ij} < r_{ij}$$

where  $j$  denotes ligand atoms,  $d_{ij}$  is the water–ligand distance squared, and  $r_{ij}$  is the sum of the ligand and water VdW radii squared. A value of 1.4 is used for the water VdW radius. The removal fraction is capped at 1.0 for complete removal. First shell waters are considered to be removed by the ligand if the respective removal fraction is  $>0.6$ . If the atom of the charged group has a first shell water removed, then the algorithm detects if the charged group is compensated for this removal by either a salt bridge between the ligand and the charged group or a hydrogen bond from the ligand to the charged protein atom. If there is no such compensation, a penalty of 4.0 kcal/mol is applied for desolvating the charged group.

Second, we describe the special penalty term, called OPRK, which was introduced into WScore to penalize disruption of a special pair of waters. It is discussed in depth in the "Model of Ligand Binding in the Kappa Opioid Receptor" section. It penalizes ligands which displace waters hydrogen bound to a special pair of waters, each with displacement free energy  $dG$  relative to bulk (as computed by the WaterMap inhomogeneous solvation algorithm; see refs 39 and 40 for details) of more than 5.5 kcal/mol and are less than 3.2 Å apart, and are not hydrogen bound to a backbone NH or CO group. In the case of KOR, we term these two special waters *water 1* and *water 2*. In `watermap_wm.mae` (provided in the Supporting Information), these waters are labeled 3 and 2, respectively. If a water in the pair is removed, a compensatory hydrogen bond to the ligand must be formed, or a penalty of 3.0 kcal/mol is applied. If neither water in the pair is removed but neighboring waters that stabilize the pair are displaced by the ligand, then a hydrogen bond to the ligand must be formed to replace their stabilization or the penalty is applied. If the pair is completely displaced, it is checked to see if either water was bound to an Asp or Glu. If this is the case and there are not sufficient other waters to solvate the side chain charge or a salt bridge is not made by the ligand, then a penalty is applied. The WScore module was run with these terms included across the entire WScore training set, and did not result in penalizing any of the  $\sim 600$  active compounds in that training set. These terms are presently included as a component of the full WScore scoring function; we focus on them here because, as noted above, they play a central role in molecular recognition in the KOR receptor.

WScore calculations were run by distributing ligands across multiple processors, using the default grid and box size parameters in Glide. WaterMap was run initially using the KOR receptor as described above, and the positions of the WaterMap waters were read into the WScore module and placed on the Glide grid. Each WScore calculation requires on the order of 10 CPU minutes on one processor, or approximately twice the CPU time of a Glide XP calculation.



Optimization of the WScore algorithms is ongoing, and we expect that the required CPU time can be reduced significantly.

**6. Free Energy Perturbation Calculations.** Free energy perturbation (FEP) calculations were performed using the Schrödinger Desmond Package.<sup>45,46</sup> The starting structure for the KOR calculation was taken from PDB ID 4DJH. The proteins were prepared using the Protein Preparation Wizard during which the protonation states were assigned assuming a pH of 7.0. The proteins together with their native ligands were then inserted into a pre-equilibrated GPCR template using the `mold_gpcr_membrane` script in Maestro, and the entire system was solvated with SPC waters. The standard membrane protein relaxation protocol in Desmond was then used to generate an equilibrated system for FEP calculations.

During the relaxation process, two short minimizations were carried out to remove the extraneous forces from the system. Next, the system was heated to a target temperature of 323 K for 60 ps and then underwent liquid equilibration. During these two stages, the protein's heavy atoms were restrained while lipids were allowed to move freely around the protein and waters were prevented from entering the hydrophobic bilayer by applying a biasing Gaussian potential, ensuring the formation of necessary interactions between the lipid head groups and the protein's polar residues. The Gaussian potentials are applied on all the water molecules on the *z* direction (the *z* direction is from the inside of the membrane to the outside of the membrane) centered on  $z = \pm 10$  Å with spread of 0.5 Å and well depth of 10 kcal/mol to prevent the water molecules from entering into the space between the lipid and the protein during these simulations. The system was further relaxed by three additional short MD simulations while the biasing potential on water was removed and the restraint on the protein was gradually turned off. The first 100 ps MD simulation was run under the NPT ensemble with solute heavy atoms restrained to their initial positions by a force constant of 10 kcal/mol/Å<sup>2</sup>. In the second MD simulation, the restrain force constant on the solute heavy atoms was slowly decreased from 10 to 2 kcal/mol/Å<sup>2</sup> during 600 ps. Then, in the third MD simulation, only the protein *C $\alpha$*  atoms were restrained and the simulation lasted for 100 ps. After these three short MD simulations, another MD simulation was run under the NPT ensemble with a total of 5 ns with no restraints, ensuring full relaxation of the system.

The last frame from the relaxation process was used as the input for FEP calculations. The GPCR and the native ligand were extracted from the last frame of the trajectory and imported into Maestro. The ligand functional group mutation module and atom mutation module implemented in Desmond were used to create the input structures for the FEP calculations. The input structure files generated from Maestro were then merged with the output Desmond cms files from the relaxation MD simulation, and the full system connection table (ct) in the cms file was generated through the Desmond `rebuild_cms` python script. The multisim input file generated from Maestro was modified by removing the `system_builder` and relaxation stages.

The OPLS2.1<sup>47,48</sup> force field was used in the FEP calculations. To get more efficient sampling, the recently developed FEP/REST method<sup>22,24</sup> implemented in Desmond was used in the production stage. The ligand atoms directly involved in the perturbation and the aromatic ring where the functional group is attaching to are included in the REST region. The FEP simulations were run with a total number of

12 lambda windows under the NPT ensemble using 4 GPU cards. The details about the FEP/REST methodology including the lambda schedule were reported in a prior publication.<sup>22–24</sup> The production stage lasted 5 ns for both the complex and the solvent simulations. Replica exchanges between neighboring  $\lambda$  windows were attempted every 1.2 ps. The Bennett acceptance ratio method (BAR)<sup>49</sup> was used to calculate the free energy, and errors were estimated using the cycle closure convergence error estimate reported in ref 46.

## ■ MODEL OF LIGAND BINDING IN THE KAPPA OPIOID RECEPTOR

**1. Motivation.** Computational ligand binding experiments that output accurate binding modes and experimentally validated approximations of binding affinities are excellent first steps in the lead discovery stage of a drug discovery project. The widely used docking program, Glide, has been tested in its ability to distinguish between known active binders and large sets of chemically similar decoys compiled by the Cavasotto group (GLL/GDD<sup>37</sup>) for several GPCR crystal structures. For a given GPCR, a list of known agonists and antagonists is provided. Each of these actives are accompanied by 39 decoys, which have similar properties—notably similar molecular weights, number of rotatable bonds and hydrogen bond donors and acceptors, and formal charge. However, decoys that are too similar to either other decoys or known actives are discarded. These ligand and decoy data sets thus present good challenges by which to assess docking scoring functions, since all of the molecules look like, at first glance, potential binders. It must be noted that the ligands are not experimentally tested for binding affinity to their respective GPCR, and while it is assumed that most are not active, it is possible that a small number could actually be. While for a few GPCRs (such as the  $\beta$ -adrenergic and histamine H1 receptors) Glide docking yielded good results (distinguishing between actives and decoys), others proved challenging. We found this to be true for the KOR as well, as Glide SP and XP were unable to effectively distinguish between the GLL/GDD data set of 23 known antagonist binders and 897 associated decoys.

To date, there is only one structure of the KOR, and out of a diverse set of active binders, it is plausible that only a subset will bind to it without major induced fit effects. However, a correct scoring function should find that at least these compounds have excellent binding free energies that outrank decoy molecules that either do not bind or bind weakly (typically in the micromolar range), and should produce good early enrichment statistics. Just how good depends on a variety of factors such as the particular set of active compounds being tested or the innate flexibility of an active site (a very rigid receptor active site will accommodate a high fraction of known active molecules with minimal structural rearrangement, whereas a single conformation of a highly flexible active site may fail to dock a very high percentage of a diverse set of active compounds). In the typical situation (which we assume here), some subset of the active compounds will fit acceptably into our existing KOR receptor structure, yielding a binding pose close to what would be found experimentally, and this should enable a properly performing scoring function (which must be able to accommodate small fluctuations of the ligand binding pose) to rank these compounds very highly compared to the decoy set. However, the early and late enrichments using both the SP and XP scoring functions in Glide to dock a set of 23 KOR antagonists and a large corresponding set of 897

decoys are worse than random and not useful for the lead discovery process, as is shown in Figure 1 below.

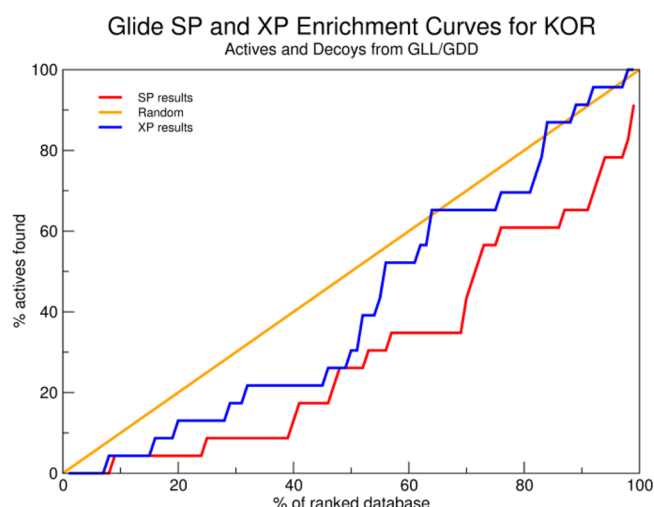


**Figure 1.** Enrichment curves of 23 actives and a corresponding decoy set from the GLL/GDD database using the SP (red) and XP (blue) scoring functions. Both are unable to discriminate between active and decoy molecules. The yellow line represents a random selection of molecules.

**2. Improving Scoring via the Inclusion of Water into the Docking Calculations.** Clearly, a modification of these scoring functions is needed to correctly model ligand binding in the experimentally determined KOR active site. The WScore scoring function is a major revision of the Glide XP scoring function in which the localized water structure in the active site, calculated using the MD-based WaterMap method,<sup>39,40</sup> is integrated into the Glide XP model. Within the rigid receptor approximation, the position of the WaterMap hydration sites is rigorously defined on the Glide XP docking grid, as is the (approximate) displacement free energy of these waters. The interaction of the ligand with the water structure can then be specified much more thoroughly than in a conventional empirical scoring function, in which only the interactions of the ligand with the protein are considered explicitly. It must be noted that, throughout this article, any reference to a specific water or hydration site refers to those acquired via a WaterMap simulation. We compare the WaterMap waters to the few crystallographic waters from the KOR PDB file in Figure 2. The bolded box encases the most important water (termed *water 1*) for understanding the binding of JD<sub>1</sub>Tic and is described in great detail in section 2.2 of the description of the model of ligand binding to KOR. The crystallographic water is only 0.4 Å away from the simulated WaterMap water. The double-lined box in Figure 2 exposes a water not found with WaterMap, probably because the presence of the hydroxyl on the ligand causes an influx of waters in the region not seen when the ligand is not present. All other crystallographic waters near the ligand are found within approximately 2 Å of WaterMap waters, which is within both the error range of WaterMap as well as movement of waters in the presence of the ligand. To account for water flexibility, there are algorithms within WScore that allow for some water movement.

An initial summary of the WScore approach, along with preliminary results for several targets using the DUD data set, has been presented in ref 17. In the present paper, we utilize

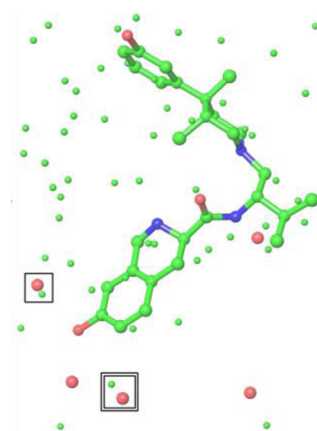


**Figure 2.** Comparison of crystallographic waters (in red) from the KOR crystal structure (PDB ID 4DJH) and WaterMap waters (in green). The bolded box encases both the WaterMap and crystallographic *water 1*, expanded upon later in the paper. The double-lined box encases a crystallographic water near the ligand that appears to have a nearby WaterMap water farther away.

the WScore scoring function in its most recent formulation but add one new term, which we call OPRK, that is important in modeling ligand binding to the KOR—essentially making possible accurate discrimination between known active antagonists and decoy molecules. The addition of OPRK to the scoring function has been tested using the standard benchmark of 25 virtual screens (each consisting of a different target receptor with multiple PDB structures) employed in the previous development of WScore. It does not adversely affect treatment of any other system that we have investigated to date. A full description of the benchmark virtual screens will be presented in a future publication.

Glide XP contains a number of terms which delineate specific molecular recognition motifs, including recessed salt bridges, displacement of hydrophobically enclosed water, and the formation of correlated hydrogen bonds in hydrophobically enclosed regions. These terms are highly effective in identifying the principal drivers of potency in known active compounds for many receptors, such as kinases.<sup>33–35</sup> However, as discussed in refs 33–35, Glide XP as originally formulated lacks terms to identify strain energy, and desolvation and trapping of water in a hydrophobic pocket by the ligand. WScore remedies the first of these deficiencies by using geometrical criteria for assigning penalties for exceptionally high energy ligand rotamer states, and the second by using interactions of the WaterMap predicted hydration sites with the ligand to assign desolvation penalties, as well as penalties for water molecules which are destabilized by additional hydrophobic contacts with the ligand.

An important point is that the WScore desolvation and ligand strain terms are not receptor specific; they are global terms, dependent upon the geometry of the protein–ligand complex and associated WaterMap hydration sites, which can be applied to an arbitrary ligand and receptor. All penalty terms that have been implemented have been tested on a large data set of ~600 protein–ligand complexes from the PDB, and avoid applying penalties to these complexes which would inappropriately reduce the score of known active compounds. Furthermore, the various terms in the model are required to be physically motivated, as opposed to arising from fitting a large number of arbitrary descriptors to experimental structure–activity relationships.

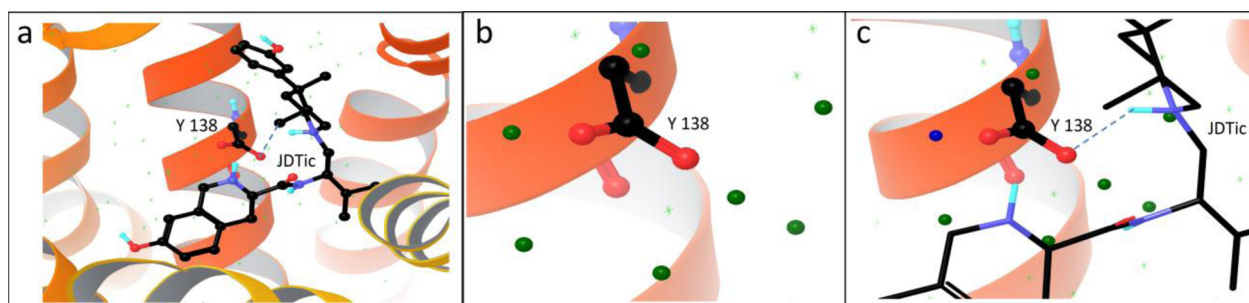


**Figure 3.** Environment of Asp 138<sup>3,32</sup> in KOR. Small green x's represent WaterMap hydration sites. Dashed blue lines represent salt bridges. (a) Salt bridge formation between JDtic and Asp 138<sup>3,32</sup> and nearby protein residues of the binding pocket. (b) Seven waters (in dark green) solvating Asp 138<sup>3,32</sup> in the absence of ligand. (c) Six waters (in dark green) displaced by JDtic, leaving only one remaining water (in dark blue), which would leave Asp 138<sup>3,32</sup> desolvated if not for the compensating salt bridges formed with basic amines.

In the present discussion, we focus on two key terms in WScore which play a critical role in discriminating active compounds from decoys in the KOR docking experiments that we have carried out. First, the great majority of known KOR tight binders have a positively charged nitrogen that likely forms a salt bridge with Asp 138<sup>3,32</sup>. Formation of this salt bridge is necessary in these cases to compensate for desolvation of Asp 138<sup>3,32</sup> by the ligand. We describe the physics underlying the WScore desolvation term which enforces this condition below; this term was already implemented in WScore, and is used in this study without further adjustment. Second, in our analysis of the WaterMap derived water structure in the KOR active site, we have uncovered a highly unusual water structure which we hypothesize plays a novel role in KOR molecular recognition. No analogue of this specific water arrangement is found in any of the other complexes in our PDB derived test suite, although similar structures may well be present in other GPCR active sites. We implement a simple but effective model to describe the effects of KOR ligand binding on this water structure, and it provides a readily understandable mechanism for discriminating active compounds from decoys in many cases.

**2.1. Desolvation Term in WScore.** A substantial fraction of charged residues in proteins place their side chains in highly solvent exposed locations, such that their solvation free energy is comparable to what is achieved in bulk solution. An alternative conformation with acceptable free energy is the formation of a salt bridge with a complementary protein residue, typically one with a significant degree of solvent exposure. Salt bridges which are recessed (i.e., have restricted solvent exposure) are also observed, typically when there are no good alternatives.

When a ligand group is proximate to a charged residue that is in bulk solution or in a salt bridge, there is generally not a highly deleterious effect on the binding free energy, even if the group is hydrophobic. In bulk solution, water molecules can reorganize around the charged atoms and construct an alternative first solvation shell. If the protein residue is in a salt bridge, solvation free energy of the charge pair is significantly smaller than that of an isolated charged residue (as the electric field is essentially now dipolar), so again, perturbations of the first shell can be tolerated as long as they are not too extreme.

However, there are cases in which a charged residue is positioned in the active site in a confined space, without making a salt bridge. WaterMap calculations on such structures frequently reveal multiple localized waters which are hydrogen

bonded to the charged side chain. Such a water structure indicates that satisfactory solvation of the side chain requires a specific water structure, as opposed to the situation in bulk solution where there are a large number of different solvent configurations with similarly favorable interactions with the charged group. Disruption of this water structure by the ligand, without forming a compensating salt bridge to the side chain, is thus much more likely to lead to a substantial loss of free energy. This hypothesis is confirmed by examination of a large number of WaterMap calculations on complexes in the PDB. There are a small number of complexes in which a single WaterMap water bound to a charged side chain is displaced without compensation but very few where more than one such water is displaced without compensation, based on our analysis of the WScore training set. Therefore, a major penalty term is assigned when a ligand causes water displacement with these characteristics.

To get a fully accurate picture of the water structure inside a protein active site from X-ray crystallography, a much higher resolution than the 2.9 Å of KOR is needed. Therefore, we cannot use exclusively experimental data to analyze the KOR water structure. Instead, we perform a WaterMap simulation in the KOR receptor with the ligand removed. Previous work demonstrates that WaterMap provides an excellent description of the location of localized water sites, as well as approximate displacement free energies for these waters, which is important in the construction of an effective scoring function.<sup>39,40</sup> We focus below on two key aspects of this water structure; the first solvation shell of Asp 138<sup>3,32</sup> and a pair of energy waters deep within the binding site that interact with a hydroxyl group of the JDtic ligand close to TMs 5 and 6.

In the KOR active site, Asp 138<sup>3,32</sup> is buried in the binding pocket and does not form a salt bridge with another protein residue. Examination of the WaterMap results reveals that Asp 138<sup>3,32</sup> is hydrogen bound to 7 WaterMap waters (see Figure 3b). Displacement of a significant number of these waters by a ligand without forming a salt bridge leads to a structure in which the charge on the Asp is desolvated and adjacent to the ligand. The penalty term described above enforces the condition that the Asp is either properly solvated or forms a salt bridge when in the presence of a bound ligand. In the KOR crystal structure, JDtic makes at least one salt bridge to Asp 138<sup>3,32</sup> (see Figure 3a). The salt bridge compensates for the fact that the ligand displaces all but one of the waters stabilizing Asp 138<sup>3,32</sup> (see Figure 3c). D138A mutagenesis experiments demonstrated an almost 100-fold reduction in the binding affinity of JDtic.<sup>50</sup> Wu et al. in fact propose that JDtic contains



two protonated amines, one in the piperidine and the other in the isoquinoline moieties, and that both form salt bridges. We believe that it is more likely that only the piperidine amine is positively charged. The piperidine and isoquinoline nitrogens are in very close proximity, only 5.1 Å distant in the crystal structure. Protonation of both states would create substantial electrostatic repulsion, and appears very unlikely to us for that reason. Consistent with this hypothesis, experiments showed that, if the isoquinoline nitrogen is replaced by a carbon, oxygen, or sulfur atom, the binding affinity is not significantly reduced.<sup>51</sup> As is noted below, the singly protonated species also yields a more accurate structure when redocked into the receptor. The docked structures of JDTic with both one and two protonated amines are provided in the Supporting Information files JDTic-docked.pdb and JDTic\_minus\_OH-docked.pdb. Further investigation of this point will require accurate calculation of the  $pK_a$  of the various JDTic nitrogen atoms, a difficult modeling task which could be investigated in future work. The issue of the JDTic protonation state is not crucial for the enrichment studies which follow.

**2.2. OPRK Term in WScore.** From our WaterMap simulations, the active site of KOR (as well as MOR and DOR and likely other GPCRs) contains a large number of hydration sites that are for the most part localized by the criterion used in the WaterMap algorithm,<sup>39,40</sup> leading to a network of water molecules forming multiple hydrogen bonds, as in the structure of ice. A WaterMap hydration site is distinguished by a number of features; first, the approximate prediction for the free energy of displacement, and second, the number of hydrogen bonds that are formed to neighboring water molecules and polar or charged protein groups. Ordinarily, when hydration sites make four hydrogen bonds, a significant number of these hydrogen bonds are with protein groups, and the water is difficult to displace in terms of free energy. However, near TMs 5 and 6, the KOR WaterMap reveals one water molecule (termed *water 1*), shown in Figure 4a, which makes four hydrogen bonds, three with other WaterMap sites and one with Tyr 139<sup>3,33</sup>, and has an extremely unfavorable (i.e., easy to displace) free energy ( $\sim 6$  kcal/mol). Such a site resembles that of a water molecule in ice at room

temperature, where the low entropy of the site leads to a very unfavorable free energy. Thus, in this region of the KOR active site, there is an unusual degree of structuring of the water molecules despite the lack of immediately proximate protein groups. In other types of receptors, binding pockets are generally smaller and narrower, so that the possibility of forming an ice-like structure is limited. In the present case, the combination of significant confinement of the water, coupled with the lack of available protein groups for *water 1* to hydrogen bond to, leads to the unusual situation described above.

The local structure in this region appears even more ice-like when one considers the fact that *water 1* is hydrogen bonded to *water 2* (see Figure 4a), which is also a highly unstable water ( $\sim 6$  kcal/mol). *Water 2* makes only three hydrogen bonds, one to *water 1*, one to another WaterMap water, and one to Asp 223<sup>5,35</sup>. No fully analogous pair of waters can be found in any of the  $\sim 600$  PDB complexes that make up the standard WScore training set (determined by scoring the native crystal structures in conjunction with all of the respective WaterMaps and not finding a pair with the numerical criteria specified in the Theoretical Methods section above).

The significance of *water 1* is suggested by Wu et al. (a water molecule is seen in this position in the experimental crystal structure 4DJH), and is further elucidated when examining the crystal structure of JDTic, or the docked poses for morphine-like actives docked into 4DJH using Glide. In the JDTic structure, the hydroxyl bound to the isoquinoline moiety makes a hydrogen bond to *water 1*, compensating for the two displaced waters previously bonded to *water 1* (see Figure 4b). If the hydroxyl is mutated to a hydrogen, experimental measurements show that 3 kcal/mol of binding affinity is lost (i.e., a 100-fold reduction in affinity).<sup>12</sup> JDTic also forms an aromatic C–H $\cdots$ O hydrogen bond to *water 1*. Docked poses of experimentally known tight binding morphine-like ligands suggest that they can make two hydrogen bonds with *water 1*, possibly leading to additional binding affinity.

Ordinarily, water-mediated hydrogen bonding is not a significant driver of potency. However, when a water molecule has the extraordinary, ice-like structure of *water 1*, loss of a hydrogen bond to another water will be very costly, because the hydrogen bond energy lost cannot be made up by either forming an alternative hydrogen bond in a different geometry or via an increase in entropy. Hence, we apply a penalty to docked poses in which *water 1* loses hydrogen bonds which are not replaced by a sufficiently favorable interaction with the ligand (this occurs when neighboring, stabilizing waters are displaced upon ligand binding). On the basis of prior experience with WScore parametrization, and taking into account the unusual features of the present structure, the expectation would be that replacement of a hydrogen bonded water with a hydrogen bond from the ligand would result in a favorable free energy gain (as the displaced water gains entropy by going into bulk solution), whereas replacement of a hydrogen bond with an aromatic C–H bond to the water would result in a mildly unfavorable free energy change (as the aromatic C–H bond is not as strong as a normal hydrogen bond, and the hydrogen bond strength is critical here due to the relative immobility of *water 1*). As many of the docked decoy molecules displace multiple waters surrounding *water 1* but fail to form any hydrogen bonds with *water 1*, this term leads to significantly improved discrimination between actives and decoys. It also helps in explaining the very tight binding of morphine, which has three oxygen atoms that can hydrogen

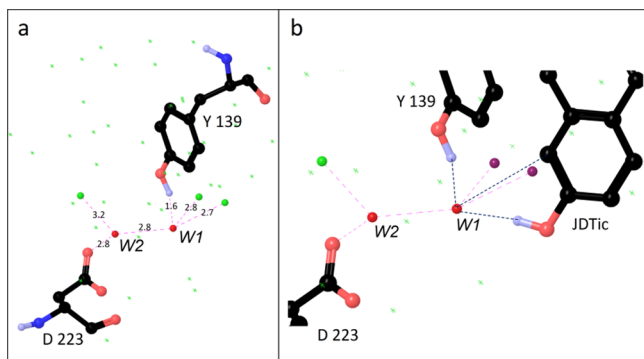


**Figure 4.** High energy water pair structure. (a) *Water 1* (W1, rightmost red) is bound to *water 2* (W2, leftmost red), Tyr 139<sup>3,33</sup>, and two other waters (rightmost greens). *Water 2* is bound to *water 1*, Asp 223<sup>5,35</sup>, and another water (leftmost green). The small green x's represent the other hydration sites in the area. All numbers over pink lines represent bond distances in Å. (b) In the presence of JDTic, two waters bound to *water 1* (in dark purple) are displaced. A compensatory hydrogen bond as well as an aromatic CH bond (both labeled with black lines) are made between *water 1* and JDTic.



bond to *water 1*, despite the small size of this molecule. Similarly, if a ligand displaces *water 1*, then a compensatory hydrogen bond to *water 2* must be made. If both waters are displaced, the ligand must form satisfactory interactions with nearby protein groups and waters. Details are given in the WScore section of the Theoretical Methods section.

## RESULTS AND DISCUSSION

**1. Self-Docking of JDTC.** Having integrated our insights from the water structure within the KOR active site into WScore, we then attempted to validate our model. To begin, we self-docked JDTC into KOR (see Figure 5) using the



**Figure 5.** Docked lowest energy pose of JDTC with two protonated amines (green) and JDTC with only one protonated amine (orange) overlaid on the crystal structure of JDTC bound to KOR (black). When JDTC contains two protonated amines, the phenol attached directly to the piperidine moiety is rotated out of the plane of the native JDTC structure.

doubly protonated state of JDTC, yielding a pose that almost exactly superimposes onto the crystal structure of the ligand, except for the phenol directly attached to the piperidine moiety. The heavy atom root-mean-square deviation (rms) between the docked and crystal structure pose is 2.8 Å, and the docking score is  $-10.6$  kcal/mol. When the nitrogen on the semi-saturated ring in the isoquinoline is neutral, the docked pose has an RMSD of 0.8 Å to the position in the crystal structure and a score of  $-11.1$  kcal/mol, which corresponds to about 1 nM binding affinity. The improved RMSD obtained for the singly protonated species provides support for this protonation state assignment, as suggested above, and we will focus on results using the singly protonated JDTC moiety in what follows. The experimental binding affinity of JDTC to the crystallized KOR with a T4 lysozyme inserted at the site of intracellular loop 3 is 0.6 nM.<sup>14</sup> In order to make an accurate comparison, the T4 lysozyme present in the crystal structure is kept during docking calculations. Docking JDTC without the isoquinoline hydroxyl group yields a score of  $-8.5$  with both amine groups protonated, and  $-8.0$  with only the piperidine amine group positively charged. A 3 kcal/mol drop in the docking score corresponds to about a 100-fold reduction in binding affinity, in good agreement with the experimental data for removing the hydroxyl group, noted above. The docked poses of JDTC with and without the hydroxyl groups are almost the same; thus, degradation in binding affinity is not a function of a different docking pose with completely new sets

of contacts. Furthermore, we also rescored the native JDTC pose without the hydroxyl and obtained a score of  $-8.2$ , confirming that the lower score of JDTC without hydroxyls is indeed coming from the removal of the hydroxyl group, and not from a different docking pose.

## 2. Cross-Docking into the KOR Crystal Structure.

Accurate redocking of a receptor's cocrystallized ligand is a necessary but not sufficient criterion to be able to pick out cross-docked known active ligands from a set of decoys. Recent literature<sup>52–55</sup> points to the idea that ensemble docking gives the best cross-docking results—a natural consequence of the fact that even similar looking ligands can induce a conformational change in the active site. There is only one crystal structure of KOR in the antagonist bound state, and it is most likely that many known antagonists will not fit into the JDTC bound structure. Thus, the terms added to the scoring function have to be flexible enough to accommodate ligands that require modest reorganization of the binding pocket; more serious reorganization will require new crystal structures with different ligands. Induced fit docking methods can also be tried but are left for investigation in subsequent work. Using the GLL/GDD data set for KOR,<sup>37</sup> we docked 23 known active antagonists and a set of decoys generated by enforcing a measure of ligand-decoy similarity of six physical properties while also requiring significant chemical dissimilarity. This provides a challenging test set for WScore, as the decoys are similar enough that they can readily be accommodated into the KOR binding site. All but 4 of the 23 actives contain a morphinan core. Note that, for this docking experiment, the JDTC ligand is not included. We chose to focus on antagonist binders because the KOR crystal structure is in an antagonist bound state. The docked structures of the active compounds are found in the Supporting Information. Each is a pdb format file whose name is a number, followed by -docked.pdb. The number corresponds to the title of the compound from the original GLL data set that can be downloaded at <http://cavasotto-lab.net/Databases/GDD/Download/>.

The results show excellent early enrichment (see Figure 6a and b) using WScore and 4DJH. Almost 40% of the actives appear in the top 3% of all docked structures (actives and decoys), and the top scoring active is outranked by no decoys. The actives with the highest binding affinities are morphinans that overlay the binding mode of JDTC and, as expected, stabilize the high energy water pair with hydrogen bonds and aromatic CH bonds, as seen in three examples in the Supporting Information. Furthermore, actives with good docking scores have a binding mode similar to those seen in the morphinan cocrystallized ligands in the MOR<sup>14</sup> and DOR<sup>13</sup> structures. This lends further experimental support to the computational docking results, as when the receptor cocrystallized ligands and KOR docked ligand poses are aligned, they are all roughly superimposed. In contrast, the previous SP and XP scoring functions yielded zero actives in the top 3% of docked structures, with 76 and 66 decoys outranking the top scoring active, respectively (see Figure 6c). Furthermore, the actives appear to be consistently misdocked, with rms deviations of the morphinan core carbon atoms as large as 7 Å. Glide with the SP and XP scoring functions also generated very few high scoring decoys that appear plausibly docked, in comparison to the JDTC and good scoring morphinan active poses. SP yielded no high scoring decoy molecules that, based on the hypotheses of our model, satisfies the requirements of binding to *water 1* or *water 2*. XP performed slightly better, with roughly a third of

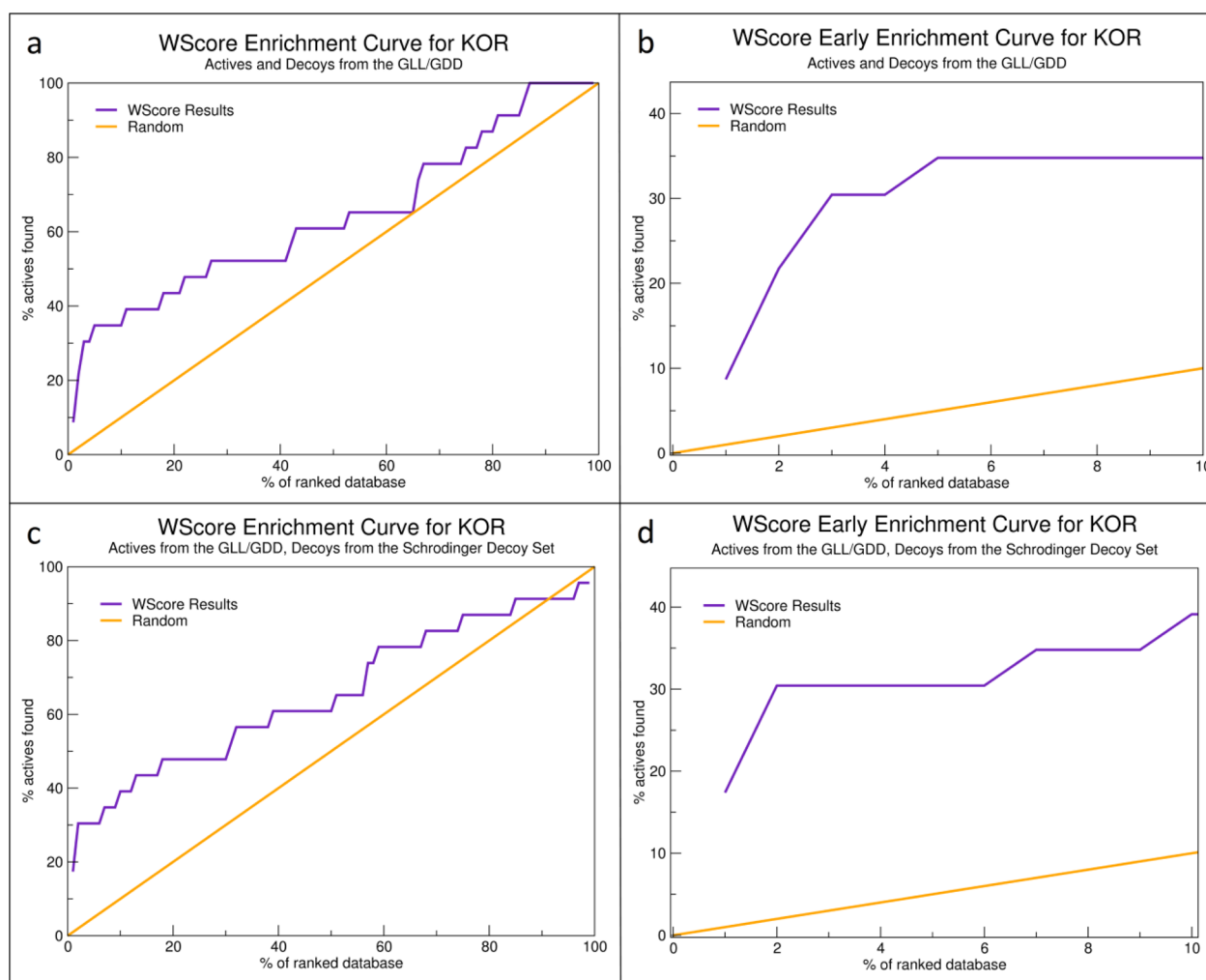


**Figure 6.** Enrichment curves obtained using WScore. (a) Enrichment against 23 active and 897 decoy molecules that were taken from the GLL/GDD database. Results are a significant improvement over the corresponding SP and XP calculations (see Figure 1). (b) The WScore early enrichment curve for the top 5% of actives and decoys using the GLL/GDD decoys. (c) Enrichment using the 23 active compounds from GLL/GDD and the Schrödinger decoys set. (d) Early enrichment for the Schrödinger decoy set.

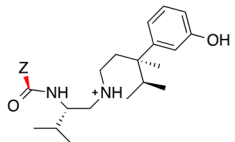
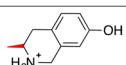
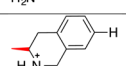
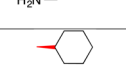
the top scoring decoys having reasonable looking docked poses from this point of view.

Of the actives with morphinan cores that have poor docking scores using WScore, only one docks in a pose that is similar to that of JDTic; the remaining actives with poor scores bind in other conformations and in different areas of the binding pocket, and most likely simply do not fit properly in the active site conformation of the currently available structure (some, for example, are very large ligands which may need an expansion of the binding site). By superimposing misdocked actives with those that we believe dock correctly, we see several parts of the misdocked molecules with obvious clashes. On the basis of our understanding of the active site, as well as parallels to the crystal structures of the cocrystallized ligands of MOR and DOR, we believe that the great majority of poorly scoring morphinan actives are misdocked. The four actives without morphinan cores are less clear, in that to date there are no experimental crystal structures to suggest their most likely binding mode. They have a strikingly different structure than the morphinans and JDTic. While we cannot know for sure, we postulate that they are misdocked and most likely require a significant rearrangement of the active site in order to fit appropriately and have a high calculated binding affinity.

Twenty decoys out of 897 decoys in total have docking scores comparable to high ranking actives ( $-9$  kcal/mol or lower). Of these, 15 have roughly the same binding mode as JDTic (many overlay it explicitly), are able to form compensatory hydrogen bonds with *waters 1* or *2*, and form a salt bridge to Asp138, and have excellent hydrophobic components to their scores. Thus, they look as if they could be active, although this can only be verified by running binding assay experiments; some are likely inactive due to subtle strain effects that are not yet addressed by WScore. As emphasized before, the set of decoy molecules is based on enforcing similarity to known binders, and it would not be surprising if a few of them are actually micromolar binders. The other five top scoring decoys overlay the piperidine moiety in JDTic. At the present time, we can only speculate as to whether or not the binding mode that overlays the piperidine moiety of JDTic is valid, based on free energy perturbation calculations (FEP) we ran. This point is discussed further below.

**3. Free Energy Perturbation Calculations.** We used the FEP module in the Schrödinger suite (19), modified to be able to accommodate the membrane surrounding KOR, to investigate each part of our water model (see Table 1). First, to investigate whether the FEP simulations were in line with a

**Table 1.** Relative Drop in Binding Affinity Due to Various Mutations to JD<sub>T</sub>ic as Compared to the Native JD<sub>T</sub>ic<sup>a</sup>

Ligand (JD <sub>T</sub> ic)	Z	dG	convergence
		predicted (kcal/mol)	error (kcal/mol)
		0.00	reference
		2.07	0.8
		5.28	1.30
	CH <sub>3</sub>	6.07	1.30

<sup>a</sup>The first mutation replaces the hydroxyl on the isoquinoline moiety with a hydrogen. The second and third mutations eliminate first the benzene ring and then the saturated ring in the isoquinoline moiety to determine the binding affinity of JD<sub>T</sub>ic where Z is a methyl group.

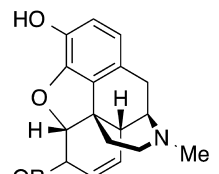
key experiment in Wu et al., we replaced the hydroxyl attached to the isoquinoline moiety with a hydrogen. On the basis of the experimental results, we expected a degradation in binding affinity of around 2–3 kcal/mol, corresponding roughly to a 100-fold reduction in binding affinity as determined experimentally.<sup>12</sup> The FEP calculations indeed produced a decrease of 2.1 kcal/mol (with a convergence error of 0.8 kcal/mol based on the cycle closure estimate<sup>22–24</sup>). This result confirms the hypothesis that the hydroxyl stabilization of the unusual water molecule in the active site of KOR is important. We then investigated whether several of the top scoring decoys that occupy only the space occupied by the piperidine moiety of JD<sub>T</sub>ic had plausible binding modes, by calculating the decrease in binding affinity when the two rings of the isoquinoline moiety are removed from JD<sub>T</sub>ic. We first removed ring 1 and saw a 5.3 kcal/mol decrease as compared to JD<sub>T</sub>ic. Removing ring 2 yielded a total of 6.1 kcal/mol decrease in binding affinity as compared to JD<sub>T</sub>ic. The 0.6 nM affinity of JD<sub>T</sub>ic corresponds to a DG of −13 kcal/mol, and a 6 kcal/mol reduction in binding affinity correlates to a score of −7 kcal/mol, or about 10 μM binding—a weak binder. Of course, WScore is not a perfect scoring function, and the five top scoring decoys that overlay the piperidine moiety in JD<sub>T</sub>ic (which roughly corresponds to removing the isoquinoline moiety) are in fact larger molecules with more chances to form good hydrophobic contacts than the JD<sub>T</sub>ic fragment that we considered in our FEP calculations. While our intuition is that these five molecules are indeed false positives (based on the fact that we are not aware of known actives which adopt this binding mode), they could conceivably be micromolar binders that happen to fall toward the top of the error range of WScore. Experimental testing would be required to investigate this possibility.

We also docked what is commonly referred to as the Schrödinger decoy set, a collection of 1000 molecules that span the space of drug-like scaffolds (available at <http://www.schrodinger.com/productpage/14/5/79/>). The enrichment graphs (for all molecules and the early enrichment) are displayed in Figure 6c and d. As with the GLL/GDD set of decoys, the top scoring molecules display binding modes that align with the JD<sub>T</sub>ic binding mode, and form the necessary interactions with *waters* 1 or 2 to keep the water region stable. The remaining top scoring molecules in the Schrödinger decoy

set overlay the piperidine portion of JD<sub>T</sub>ic. None of them are bound to a different location in the active site, or are obviously misdocked.

**4. Ligand Binding Comparison between KOR and MOR.** Lastly, we compare ligand binding in the kappa and mu opioid receptors. We calculated the WaterMap water structure for MOR and saw that there is a single high energy and extremely isolated water near TMs 5 and 6. When the WaterMap structures of KOR and MOR are superimposed, we see that this isolated water in MOR occupies almost exactly the same space as *water* 1 in the KOR water structure. Furthermore, there is a hydroxyl group on the cocrystallized ligand, β-funaltrexamine (β-FNA), in the MOR crystal structure, that hydrogen bonds to this high energy water. We hypothesize that stabilizing this water is important, just like stabilization of the high energy water pair found in KOR appears to be imperative for some ligand binding. Experiments from a study<sup>56</sup> comparing the relative binding affinities of morphine derivatives that are very potent agonists to MOR and KOR also show that the presence of a hydroxyl is important for ligand binding to both receptors. As seen in Table 2, in

**Table 2.** Experimental Binding Affinities of Morphine and Two Derivatives<sup>a</sup>

Ligand	R	KOR (μM)	MOR (μM)
	H (Morphine)	0.047±0.003	0.0018±0.0006
	C <sub>6</sub> H <sub>5</sub> O <sub>5</sub>	15±8.7	0.36±0.05
	CH <sub>3</sub>	8.0±2.5	0.35±0.11

<sup>a</sup>These data support the hypothesis that the presence of a hydroxyl (R = H) is very important for morphinan ligand binding in both KOR and MOR.

morphine (and its derivatives), there is a hydroxyl that we believe, based on docking morphine and codeine into KOR, can stabilize *water* 1, or, by our hypothesis, the high energy water in MOR. Furthermore, this hydroxyl in morphine is in the same position as the hydroxyls in JD<sub>T</sub>ic and β-FNA, as seen when all three are superimposed. When this hydroxyl is mutated to C<sub>6</sub>H<sub>5</sub>O<sub>5</sub>, binding is about 500 times worse, while if it is substituted with a methyl group, it is about 200 times worse. When the same two substitutions are made and binding affinity to MOR is assayed, there is a 200-fold reduction in binding affinity for both. Thus, in both opioid receptors, there is clearly binding sensitivity to the presence of a hydroxyl. Although the importance of the water structure in MOR seems plausible, we do not yet understand the difference between the pair and this single water, or why this single water might behave differently from other bridging waters in the WScore training set, and we leave this investigation for future work.

Overall, this study emphasizes the importance of the water structure within an active site. Generally speaking, displacing unstable waters which are hydrophobically enclosed increases the free energy of a system, as long as the ligand replaces the water with hydrophobic groups or appropriate ligand–receptor hydrogen bonds. Without these explicit waters present in the docking process, it is much harder to estimate such energy gains from water displacement. In the present case, the key observation is that, because of the unusual water structure,



instability of water molecules primarily is not from hydrophobic enclosure (as is typical in most enzymatic active sites) but rather due to entropic effects in a deep part of a large pocket, where the water structure is localized into an ice-like formation. By modeling the effects of water displacement in this structure, we require that any such water displacement be compensated by adequate favorable interactions, and thus incorporate a key molecular recognition element into WScore which yields a dramatically improved early enrichment for KOR virtual screening.

## CONCLUSIONS

The formation of a salt bridge being key to ligand binding for the KOR appears to follow other GPCRs, but like most receptors, there is a second piece of the binding regulation puzzle: a high energy water pair that must be kept stabilized or else a ligand cannot favorably bind. This picture is supported by experiment but for the first time analyzed with a detailed molecular explanation leading to the specific hypothesis outlined in this paper. Furthermore, we now have integrated our ligand binding motifs into WScore, which is able to pick out active ligands from similar decoys that fit in a given conformation of the receptor. Decoys that get high docking scores primarily look like reasonable weak binders. Combined, these represent a powerful tool set to embark on new drug-discovery projects aimed at the KOR.

## ASSOCIATED CONTENT

### Supporting Information

A figure depicting the docked poses of the three top scoring actives is presented. It illustrates the importance of the high energy water pair incorporated in the ligand binding model. Structure files in pdb format are included for the GLL ligands and the cocrystallized KOR ligand, JD<sub>Tic</sub>. The WaterMap file that corresponds to KOR is provided as well. This material is available free of charge via the Internet at <http://pubs.acs.org>.

## AUTHOR INFORMATION

### Corresponding Author

\*Phone: 212-854-7606. Fax: 212-854-7454. E-mail: [rich@chem.columbia.edu](mailto:rich@chem.columbia.edu).

### Present Address

<sup>§</sup>Department of Chemistry & Biochemistry, Department of Pharmacology, University of California, San Diego, CA 92093, United States.

### Notes

The authors declare the following competing financial interest(s): Richard A. Friesner has a significant financial stake in Schrodinger, Inc., is a consultant to Schrodinger, Inc., and is on the Scientific Advisory Board of Schrodinger, Inc.

## ACKNOWLEDGMENTS

We would like to acknowledge Shulu Feng for his helpful input to this project.

## REFERENCES

(1) Sproule, B.; Brands, B.; Li, S.; Catz-Biro, L. Changing Patterns in Opioid Addiction: Characterizing Users of Oxycodone and Other Opioids. *Can. Fam. Physician* **2009**, *55*, 68–69.  
(2) Center for Substance Abuse Treatment. *Medication-Assisted Treatment for Opioid Addiction in Opioid Treatment Programs*, Rockville, MD, 2005.

(3) DeLander, G. E.; Portoghese, P. S.; Takemori, A. E. Role of Spinal Mu Opioid Receptors in the Development of Morphine Tolerance and Dependence. *J. Pharmacol. Exp. Ther.* **1984**, *231*, 91–96.  
(4) Fields, H. L. Understanding How Opioids Contribute to Reward and Analgesia. *Reg. Anesth. Pain Med.* **2007**, *32*, 242–246.  
(5) Nagase, H. Chemistry of Opioids. Preface. *Top. Curr. Chem.* **2011**, *299*, ix–xi.  
(6) Nagase, H.; Fujii, H. Opioids in Preclinical and Clinical Trials. *Top. Curr. Chem.* **2011**, *299*, 29–62.  
(7) Vanderah, T. W. Delta and Kappa Opioid Receptors as Suitable Drug Targets for Pain. *Clin. J. Pain* **2010**, *26* (Suppl. 10), S10–S15.  
(8) Wang, Y. H.; Sun, J. F.; Tao, Y. M.; Chi, Z. Q.; Liu, J. G. The Role of Kappa-Opioid Receptor Activation in Mediating Antinociception and Addiction. *Acta Pharmacol. Sin.* **2010**, *31*, 1065–1070.  
(9) Bruchas, M. R.; Chavkin, C. Kinase Cascades and Ligand-Directed Signaling at the Kappa Opioid Receptor. *Psychopharmacology (Berlin)* **2010**, *210*, 137–147.  
(10) Rives, M. L.; Rossillo, M.; Liu-Chen, L. Y.; Javitch, J. A. 6'-Guanidinonaltrindole (6'-Gnti) Is a G Protein-Biased Kappa-Opioid Receptor Agonist That Inhibits Arrestin Recruitment. *J. Biol. Chem.* **2012**, *287*, 27050–27054.  
(11) Chavkin, C. The Therapeutic Potential of Kappa-Opioids for Treatment of Pain and Addiction. *Neuropsychopharmacology* **2011**, *36*, 369–370.  
(12) Wu, H.; Wacker, D.; Mileni, M.; Katritch, V.; Han, G. W.; Vardy, E.; Liu, W.; Thompson, A. A.; Huang, X. P.; Carroll, F. I.; et al. Structure of the Human Kappa-Opioid Receptor in Complex with JD<sub>Tic</sub>. *Nature* **2012**, *485*, 327–332.  
(13) Granier, S.; Manglik, A.; Kruse, A. C.; Kobilka, T. S.; Thian, F. S.; Weis, W. I.; Kobilka, B. K. Structure of the Delta-Opioid Receptor Bound to Naltrindole. *Nature* **2012**, *485*, 400–404.  
(14) Manglik, A.; Kruse, A. C.; Kobilka, T. S.; Thian, F. S.; Mathiesen, J. M.; Sunahara, R. K.; Pardo, L.; Weis, W. I.; Kobilka, B. K.; Granier, S. Crystal Structure of the Micro-Opioid Receptor Bound to a Morphinan Antagonist. *Nature* **2012**, *485*, 321–326.  
(15) Thompson, A. A.; Liu, W.; Chun, E.; Katritch, V.; Wu, H.; Vardy, E.; Huang, X. P.; Trapella, C.; Guerrini, R.; Calo, G.; et al. Structure of the Nociceptin/Orphanin Fq Receptor in Complex with a Peptide Mimetic. *Nature* **2012**, *485*, 395–399.  
(16) Fanelli, F.; De Benedetti, P. G. Update 1 Of: Computational Modeling Approaches to Structure-Function Analysis of G Protein-Coupled Receptors. *Chem. Rev.* **2011**, *111*, PR438–535.  
(17) Repasky, M. P.; Murphy, R. B.; Banks, J. L.; Greenwood, J. R.; Tubert-Brohman, I.; Bhat, S.; Friesner, R. A. Docking Performance of the Glide Program as Evaluated on the Astex and Dund datasets: A Complete Set of Glide Sp Results and Selected Results for a New Scoring Function Integrating Watermap and Glide. *J. Comput.-Aided Mol. Des.* **2012**, *26*, 787–799.  
(18) Verdonk, M. L.; Chessari, G.; Cole, J. C.; Hartshorn, M. J.; Murray, C. W.; Nissink, J. W.; Taylor, R. D.; Taylor, R. Modeling Water Molecules in Protein-Ligand Docking Using Gold. *J. Med. Chem.* **2005**, *48*, 6504–6515.  
(19) Roberts, B. C.; Mancera, R. L. Ligand-Protein Docking with Water Molecules. *J. Chem. Inf. Model.* **2008**, *48*, 397–408.  
(20) Schneider, N.; Hindle, S.; Lange, G.; Klein, R.; Albrecht, J.; Briem, H.; Beyer, K.; Claussen, H.; Gastreich, M.; Lemmen, C.; et al. Substantial Improvements in Large-Scale Redocking and Screening Using the Novel Hyde Scoring Function. *J. Comput.-Aided Mol. Des.* **2012**, *26*, 701–723.  
(21) Mason, J. S.; Bortolato, A.; Congreve, M.; Marshall, F. H. New Insights from Structural Biology into the Druggability of G Protein-Coupled Receptors. *Trends Pharmacol. Sci.* **2012**, *33*, 249–260.  
(22) Wang, L.; Berne, B. J.; Friesner, R. A. On Achieving High Accuracy and Reliability in the Calculation of Relative Protein-Ligand Binding Affinities. *Proc. Natl. Acad. Sci. U.S.A.* **2012**, *109*, 1937–1942.  
(23) Wang, L.; D, Y.; Knight, J. L.; Wu, Y.; Kim, B.; Sherman, W.; Shelley, J. C.; Lin, T.; Abel, R. Modeling Local Structural Rearrangements Using Fep/Rest: Application to Relative Binding

Affinity Predictions of Cdk2 Inhibitors. *J. Chem. Theory Comput.* **2013**, *9*, 1282–1293.

(24) Wang, L.; Friesner, R. A.; Berne, B. J. Replica Exchange with Solute Scaling: A More Efficient Version of Replica Exchange with Solute Tempering (Rest2). *J. Phys. Chem. B* **2011**, *115*, 9431–9438.

(25) Katritch, V.; Kufareva, I.; Abagyan, R. Structure Based Prediction of Subtype-Selectivity for Adenosine Receptor Antagonists. *Neuropharmacology* **2011**, *60*, 108–115.

(26) Katritch, V.; Jaakola, V. P.; Lane, J. R.; Lin, J.; Ijzerman, A. P.; Yeager, M.; Kufareva, I.; Stevens, R. C.; Abagyan, R. Structure-Based Discovery of Novel Chemotypes for Adenosine a(2a) Receptor Antagonists. *J. Med. Chem.* **2010**, *53*, 1799–1809.

(27) Carlsson, J.; Yoo, L.; Gao, Z. G.; Irwin, J. J.; Shoichet, B. K.; Jacobson, K. A. Structure-Based Discovery of A2a Adenosine Receptor Ligands. *J. Med. Chem.* **2010**, *53*, 3748–3755.

(28) Mysinger, M. M.; Weiss, D. R.; Ziarek, J. J.; Gravel, S.; Doak, A. K.; Karpik, J.; Heveker, N.; Shoichet, B. K.; Volkman, B. F. Structure-Based Ligand Discovery for the Protein-Protein Interface of Chemokine Receptor Cxcr4. *Proc. Natl. Acad. Sci. U.S.A.* **2012**, *109*, 5517–5522.

(29) Kruse, A. C.; Weiss, D. R.; Rossi, M.; Hu, J.; Hu, K.; Eitel, K.; Gmeiner, P.; Wess, J.; Kobilka, B. K.; Shoichet, B. K. Muscarinic Receptors as Model Targets and Antitargets for Structure-Based Ligand Discovery. *Mol. Pharmacol.* **2013**, *84*, 528–540.

(30) de Graaf, C.; Kooistra, A. J.; Vischer, H. F.; Katritch, V.; Kuijter, M.; Shiroishi, M.; Iwata, S.; Shimamura, T.; Stevens, R. C.; de Esch, I. J.; et al. Crystal Structure-Based Virtual Screening for Fragment-Like Ligands of the Human Histamine H(1) Receptor. *J. Med. Chem.* **2011**, *54*, 8195–8206.

(31) Kolb, P.; Rosenbaum, D. M.; Irwin, J. J.; Fung, J. J.; Kobilka, B. K.; Shoichet, B. K. Structure-Based Discovery of Beta2-Adrenergic Receptor Ligands. *Proc. Natl. Acad. Sci. U.S.A.* **2009**, *106*, 6843–6848.

(32) Negri, A.; Rives, M. L.; Caspers, M. J.; Prisinzano, T. E.; Javitch, J. A.; Filizola, M. Discovery of a Novel Selective Kappa-Opioid Receptor Agonist Using Crystal Structure-Based Virtual Screening. *J. Chem. Inf. Model.* **2013**, *53*, 521–526.

(33) Friesner, R. A.; Murphy, R. B.; Repasky, M. P.; Frye, L. L.; Greenwood, J. R.; Halgren, T. A.; Sanschagrin, P. C.; Mainz, D. T. Extra Precision Glide: Docking and Scoring Incorporating a Model of Hydrophobic Enclosure for Protein-Ligand Complexes. *J. Med. Chem.* **2006**, *49*, 6177–6196.

(34) Halgren, T. A.; Murphy, R. B.; Friesner, R. A.; Beard, H. S.; Frye, L. L.; Pollard, W. T.; Banks, J. L. Glide: A New Approach for Rapid, Accurate Docking and Scoring. 2. Enrichment Factors in Database Screening. *J. Med. Chem.* **2004**, *47*, 1750–1759.

(35) Friesner, R. A.; Banks, J. L.; Murphy, R. B.; Halgren, T. A.; Klicic, J. J.; Mainz, D. T.; Repasky, M. P.; Knoll, E. H.; Shelley, M.; Perry, J. K.; et al. Glide: A New Approach for Rapid, Accurate Docking and Scoring. 1. Method and Assessment of Docking Accuracy. *J. Med. Chem.* **2004**, *47*, 1739–1749.

(36) Sastry, G. M.; Adzhigirey, M.; Day, T.; Annabhimoju, R.; Sherman, W. Protein and Ligand Preparation: Parameters, Protocols, and Influence on Virtual Screening Enrichments. *J. Comput.-Aided Mol. Des.* **2013**, *27*, 221–234.

(37) Gatica, E. A.; Cavasotto, C. N. Ligand and Decoy Sets for Docking to G Protein-Coupled Receptors. *J. Chem. Inf. Model.* **2012**, *52*, 1–6.

(38) LigPrep, version 2.3; Schrödinger, LLC: New York, 2009.

(39) Abel, R.; Young, T.; Farid, R.; Berne, B. J.; Friesner, R. A. Role of the Active-Site Solvent in the Thermodynamics of Factor Xa Ligand Binding. *J. Am. Chem. Soc.* **2008**, *130*, 2817–2831.

(40) Young, T.; Abel, R.; Kim, B.; Berne, B. J.; Friesner, R. A. Motifs for Molecular Recognition Exploiting Hydrophobic Enclosure in Protein-Ligand Binding. *Proc. Natl. Acad. Sci. U.S.A.* **2007**, *104*, 808–813.

(41) Jacobson, M. P.; Friesner, R. A.; Xiang, Z. X.; Honig, B. On the Role of the Crystal Environment in Determining Protein Side-Chain Conformations. *J. Mol. Biol.* **2002**, *320*, 597–608.

(42) Lazaridis, T. Inhomogeneous Fluid Approach to Solvation Thermodynamics. 1. Theory. *J. Phys. Chem. B* **1998**, *102*, 3531–3541.

(43) Lazaridis, T. Inhomogeneous Fluid Approach to Solvation Thermodynamics. 2. Applications to Simple Fluids. *J. Phys. Chem. B* **1998**, *102*, 3542–3550.

(44) Wang, L.; Berne, B. J.; Friesner, R. A. Ligand Binding to Protein-Binding Pockets with Wet and Dry Regions. *Proc. Natl. Acad. Sci. U.S.A.* **2011**, *108*, 1326–1330.

(45) Shivakumar, D.; Williams, J.; Wu, Y. J.; Damm, W.; Shelley, J.; Sherman, W. Prediction of Absolute Solvation Free Energies Using Molecular Dynamics Free Energy Perturbation and the Opls Force Field. *J. Chem. Theory Comput.* **2010**, *6*, 1509–1519.

(46) Guo, Z. J.; Mohanty, U.; Noehre, J.; Sawyer, T. K.; Sherman, W.; Krilov, G. Probing the Alpha-Helical Structural Stability of Stapled P53 Peptides: Molecular Dynamics Simulations and Analysis. *Chem. Biol. Drug Des.* **2010**, *75*, 348–359.

(47) Jorgensen, W. L.; Maxwell, D. S.; TiradoRives, J. Development and Testing of the Opls All-Atom Force Field on Conformational Energetics and Properties of Organic Liquids. *J. Am. Chem. Soc.* **1996**, *118*, 11225–11236.

(48) Jorgensen, W. L.; Tiradorives, J. The Opls Potential Functions for Proteins - Energy Minimizations for Crystals of Cyclic-Peptides and Crambin. *J. Am. Chem. Soc.* **1988**, *110*, 1657–1666.

(49) Bennett, C. H. Efficient Estimation of Free-Energy Differences from Monte-Carlo Data. *J. Comput. Phys.* **1976**, *22*, 245–268.

(50) Wu, H.; Wacker, D.; Mileni, M.; Katritch, V.; Han, G. W.; Vardy, E.; Liu, W.; Thompson, A. A.; Huang, X. P.; Carroll, F. I.; et al. Structure of the Human Kappa-Opioid Receptor in Complex with JDTic. *Nature* **2012**, *485*, 327–332.

(51) Runyon, S. P.; Brieady, L. E.; Mascarella, S. W.; Thomas, J. B.; Navarro, H. A.; Howard, J. L.; Pollard, G. T.; Carroll, F. I. Analogues of (3r)-7-Hydroxy-N-[(1s)-1-[[[(3r,4r)-4-(3-Hydroxyphenyl)-3,4-Dimethyl-1-Piperidinyl ]Methyl]-2-Methylpropyl)-1,2,3,4-Tetrahydro-3-Isoquinolinecarboxamide (JDTic). Synthesis and in Vitro and in Vivo Opioid Receptor Antagonist Activity. *J. Med. Chem.* **2010**, *53*, 5290–5301.

(52) Rao, S.; Sanschagrin, P. C.; Greenwood, J. R.; Repasky, M. P.; Sherman, W.; Farid, R. Improving Database Enrichment through Ensemble Docking. *J. Comput.-Aided Mol. Des.* **2008**, *22*, 621–627.

(53) Rueda, M.; Bottegoni, G.; Abagyan, R. Recipes for the Selection of Experimental Protein Conformations for Virtual Screening. *J. Chem. Inf. Model.* **2010**, *50*, 186–193.

(54) Craig, I. R.; Essex, J. W.; Spiegel, K. Ensemble Docking into Multiple Crystallographically Derived Protein Structures: An Evaluation Based on the Statistical Analysis of Enrichments. *J. Chem. Inf. Model.* **2010**, *50*, 511–524.

(55) Nichols, S. E.; Baron, R.; Ivetac, A.; McCammon, J. A. Predictive Power of Molecular Dynamics Receptor Structures in Virtual Screening. *J. Chem. Inf. Model.* **2011**, *51*, 1439–1446.

(56) Mignat, C.; Wille, U.; Ziegler, A. Affinity Profiles of Morphine, Codeine, Dihydrocodeine and Their Glucuronides at Opioid Receptor Subtypes. *Life Sci.* **1995**, *56*, 793–799.